J|A|C|S
COMMUNICATIONS

Highly Active and Robust Cp* Iridium Complexes for Catalytic Water Oxidation

Jonathan F. Hull,[†] David Balcells,[‡] James D. Blakemore,[†] Christopher D. Incarvito,[†]
Odile Eisenstein,[*,‡] Gary W. Brudvig,[*,†] and Robert H. Crabtree[*,†]

Chemistry Department, Yale University, P.O. Box 208107, New Haven, Connecticut 06520, and Université Montpellier 2, Institut Charles Gerhardt, CNRS 5253, cc 15001, Place Eugène Bataillon 34095, Montpellier, France

Received February 18, 2009; E-mail: robert.crabtree@yale.edu; gary.brudvig@yale.edu; odile.eisenstein@univ-montp2.fr

Catalytic water oxidation (eq 1) is of fundamental importance to natural and artificial photosynthesis,[1] as well as photochemical energy storage and fuel production.

$$2H_2O \xrightarrow{\text{catalyst}} O_2 + 4H^+ + 4e^- \qquad (1)$$

Few homogeneous water oxidizing catalysts are known. Ones that contain Ru, Mn, or Ir have been reported,[2] but high activity and stability are often lacking. A few are only active with $2e^-$ primary oxidants, such as oxone or OCl^-. Ones active with Ce(IV) are more significant, being more relevant to the $4 \times 1e^-$ process of photosynthesis. We now describe several robust water oxidation catalysts using Ce(IV) as the primary oxidant that are the most active yet reported, achieving an initial rate of 54 turnover/min, and are active for several hours.

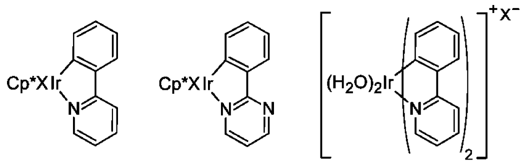

1a, X = Cl
1b, X = OTf

2, X = Cl

3, X = OTf

Figure 1. Iridium catalysts for water oxidation.

Bernhard et al.[2i] have recently reported a robust homogeneous Ir catalyst, **3** in Figure 1, that maintains activity with Ce(IV) for 1 week. Having confirmed this result, we moved to complexes with much more strongly donating ligand sets to look for improved activity and now report **1a**−**b** and **2** as highly active catalyst precursors for water oxidation, easily accessible from commercially available $[Cp^*IrCl_2]_2$.[3] The crystal structure of **2**, shown in Figure 2, confirms the expected atom connectivity.

Complex **1a** dissolves in water (50 mM), but only on addition of excess Ce(IV) in the form of CAN (cerium ammonium nitrate), and gas bubbles are observed within 1 min. For oxygen detection by the Clark electrode, bubble formation has to be avoided, so rate data for the reaction were obtained under the dilute conditions noted in Figure 3 by adding catalyst (10 μL, 38 nmol) dissolved in a $MeCN/H_2O$ mixture to the Ce(IV) solution (7 mL, 78 mM). This shows initial oxygen evolution rates for **1a**, **2**, and **3** in water with CAN, and no lag time is observed upon injection of the catalyst. Complex **1a** (54 turnover/min) and **2** (17 turnover/min) are significantly more active than the known **3** (3 turnover/min) and more active by at least an order of magnitude than those shown in Table 1. Because reaction is so fast, measurements using the Clark electrode being limited to 1 min, dilatometry was used for measurements over longer periods (see Supporting Information, SI). Gas evolution continues over 7.5 h.[4] The rate over 7 h is lower ($0.1\ s^{-1}$) than the initial rate, consistent with most catalysts reported in Table 1.

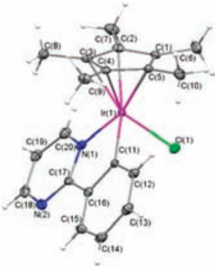

Figure 2. ORTEP diagram of **2** (see Supporting Information for XRD data).

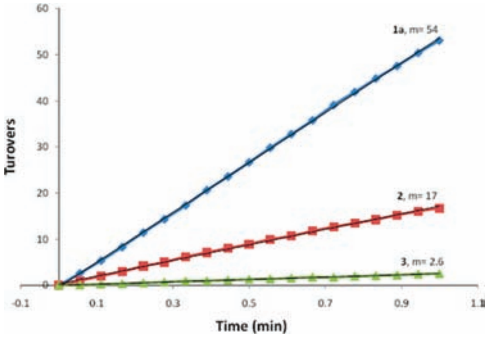

Figure 3. Initial rates for catalysts **1a**, **2**, and **3** as measured by a Clark electrode using 38 nmol (5.43 μM) of catalyst and 0.55 mmol (78 mM) of CAN in H_2O (7 mL) at 25 °C.

Cyclic voltammetry (CV) of the chloro complex **1a** in MeCN shows three irreversible oxidation waves in contrast to triflato complex **1b** which only shows two peaks. This, together with the much greater rate seen for **1a** versus **1b** (see SI), suggests that chloride oxidation may accelerate O_2 evolution via oxidation to OCl^{-5} or Cl_2.[6] This is consistent with previous reports of an accelerating effect of Cl^- ion.[7] However, we see 11.9 turnover/min from the triflate complex **1b**, so Cl^- is not required for activity. The $[Cp^*IrCl_2]_2$ dimer also evolves O_2, albeit at a much slower rate (8 turnover/min). The formation of IrO_2 or other heterogeneous catalyst is unlikely: the catalyst can be fully recovered from the reaction mixture (NMR), no lag phase is seen, no dark deposit is

---

[†] Yale University.
[‡] Université Montpellier 2.

10.1021/ja901270f CCC: $40.75

formed, evolution is reproducible, and the reaction is first order in **1b**. Furthermore, the reported reaction rate catalyzed by IrO_2 is very slow (Table 1, entry 8). Other homogeneity tests are reported in the SI. Water was confirmed as the source of O by the detection of $^{36}O_2$ in ^{18}O labeling experiments.

Assuming the chelate remains bidentate, **1**−**2** only have one labile site. If so, this limits the mechanistic possibilities and the steric bulk present may inhibit μ-oxo dimer formation or other bimolecular deactivation processes.

Moving from the pyridine complex **1a** to the pyrimidine complex **2** causes a rate decrease. Pyrimidines are less donor than pyridines, and at low pH they can also protonate at the distal N. The need for strong donor ligands is consistent with a requirement for easy attainment of a high oxidation state intermediate, plausibly an Ir^{V} oxo. A $2e^-$ oxidation from Ir^{III} is also consistent with the presence of two oxidation waves in the CV for **1b** in MeCN (see SI).

Table 1. Dioxygen Evolution Rates for Reported Homogeneous Water Oxidation Catalysts That Use Ce(IV) As Oxidant

catalyst	rate[a]	turnover/h[b]	C[c]	ref
1a	9100	>1500/5.5[d]	5.4	this work
2	2800	213/2.5[e]	5.4	this work
3	50[f]	2490/168	300	2i
$[Ru_2(bpy)_4(H_2O)_2O]^{4+}$	42	5/2	300	2a, 2h
$[Ru_2(bpp)(trpy)_2(H_2O)_2]^{3+}$	140	19/48	914	2g
$[Ru_2(npp)(4\text{-Me-py})_4Cl]^{3+}$	7.7	3200/15	333[g]	2j
$[[Ru(tpy)(pynap)Cl]^+$	340[g]	1170/20	67	2l
IrO_2 (heterogeneous)	14	na	na	2h

[a] Initial rate in (turnover/s) × 10^4. [b] Total turnover/time (h). [c] Catalyst concentration (μM). [d] By dilatometry using 1.15 M Ce(IV) and 2.90 μM **1a**. See text and SI for details. [e] By dilatometry using 1.15 M Ce(IV) and 3.09 μM catalyst. [f] We find 0.042 turnover/s with 5.4 μM catalyst. [g] Calculated from ref using our scale.

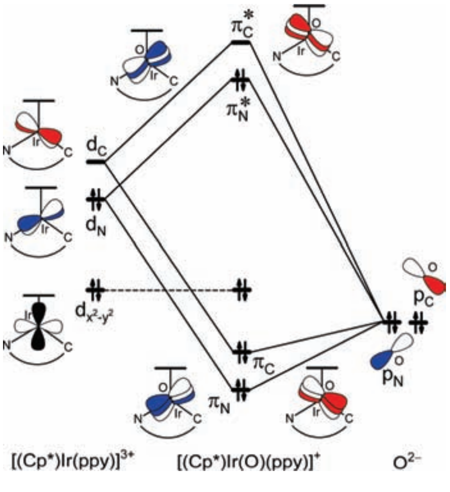

Figure 4. Qualitative interaction diagram for the molecular orbitals of $[(Cp^*)Ir(O)(ppy)]^+$ with Ir d and O p contributions.

The minimum number of metal atoms required for water oxidation is debated, but several reports[2c,i,k,l] suggest that a single metal is sufficient. The reaction is first order with respect to **1b** in the 1−80 μM range (see SI). This makes $[(Cp^*)Ir(O)(ppy)]^+$ a plausible intermediate. DFT calculations[8] show that the electronic structure of this pseudo-octahedral $(t_{2\,g})^4$ complex can be understood by the formal combination of the $[(Cp^*)Ir(ppy)]^{3+}$ and O^{2-} fragments (Figure 4).[9] The electrons on the metal are localized in the nonbonding $d_{x^2-y^2}$ orbital, which does not interact with O p orbitals. The Ir d orbitals oriented toward N, d_N, and C, d_C, make d_π/p_π interactions with the O p orbitals, yielding two bonding π(Ir=O) orbitals, π_N and π_C, and two antibonding π^*(Ir=O) orbitals, π^*_N and π^*_C. In the singlet state, π^*_N is doubly occupied and π^*_C is empty, whereas, in the triplet, both orbitals are half occupied. The presence of low-lying π^*(Ir=O) orbitals, which have a significant O contribution, may promote the formation of an O−O bond by nucleophilic attack to the oxo group, which is the key step in water oxidation.[10,11] The singlet state is only 3.7 kcal mol^{-1} above the triplet, due to the similar energies of the π^*_N and π^*_C orbitals. The accessibility of the singlet state may also facilitate the O−O bond formation, because the addition of the nucleophile will yield a diamagnetic Ir^{III} octahedral complex. The electronic structure of $[(Cp^*)Ir(O)(ppy)]^+$ is consistent with this complex being the active species of the catalytic system. A thorough experimental and theoretical investigation is now in progress.

Acknowledgment. R.H.C, G.W.B., and J.F.H. acknowledge the NSF (CHE-0614403) and NIH (GM32715) for funding. D.B. thanks Sanofi-Aventis for a postdoctoral fellowship. We thank J. N. Harvey for helpful discussions.

Supporting Information Available: Synthesis and characterization of compounds **1a**−**b** and **2**, and crystal parameters. Experimental details for oxygen evolution and kinetic measurements, CV and homogeneity tests. Optimized geometries and energies of the singlet and triplet states of $[(Cp^*)Ir(O)(ppy)]^+$. Frontier molecular orbitals of the singlet. This material is available free of charge via the Internet at http://pubs.acs.org.

References

(1) (a) Alstrum-Acevedo, J. H.; Brennaman, M. K.; Meyer, T. J. *Inorg. Chem.* **2005**, *44*, 6802. (b) Yagi, M.; Kaneko, K. *Chem. Rev.* **2001**, *101*, 21. (c) Cady, C. W.; Crabtree, R. H.; Brudvig, G. W. *Coord. Chem. Rev.* **2008**, *252*, 444.

(2) (a) Gersten, S. W.; Samuels, J. G.; Meyer, T. J. *J. Am. Chem. Soc.* **1982**, *104*, 4029. (b) Liu, F.; Concepcion, J. J.; Jurss, J. W.; Cardolaccia, T.; Templeton, J. L.; Meyer, T. J. *Inorg. Chem.* **2008**, *47*, 1727. (c) Concepcion, J. J.; Jurss, J. W.; Templeton, J. L.; Meyer, T. J. *J. Am. Chem. Soc.* **2008**, *130*, 16462. (d) Limburg, J.; Vrettos, J. S.; Liable-Sands, L. M.; Rheingold, A. L.; Crabtree, R. H.; Brudvig, G. W. *Science* **1999**, *283*, 1524. (e) Limburg, J.; Vrettos, J. S.; Chen, H.; de Paula, J. C.; Crabtree, R. H.; Brudvig, G. W. *J. Am. Chem. Soc.* **2001**, *123*, 423. (f) Tagore, R.; Crabtree, R. H.; Brudvig, G. W. *Inorg. Chem.* **2008**, *47*, 1815. (g) Sens, C.; Romero, I.; Rodriguez, M.; Llobet, A.; Parella, T.; Benet-Buchholz, J. *J. Am. Chem. Soc.* **2004**, *126*, 7798. (h) Nagoshi, K.; Yamashita, S.; Yagi, M.; Kaneko, M. *J. Mol. Catal. A* **1999**, *144*, 71. (i) McDaniel, N. D.; Coughlin, F. J.; Tinker, L. L.; Bernhard, S. *J. Am. Chem. Soc.* **2008**, *130*, 210. (j) Zong, R.; Thummel, R. P. *J. Am. Chem. Soc.* **2005**, *127*, 12802. (k) Deng, Z.; Tseng, H.-W.; Zong, R.; Wang, D.; Thummel, R. P. *Inorg. Chem.* **2008**, *47*, 1835. (l) Tseng, H.-W.; Zong, R.; Muckerman, J. T.; Thummel, R. P. *Inorg. Chem.* **2008**, *47*, 11763. (m) Geletii, Y. V.; Botar, B.; Kogerler, P.; Hillesheim, D. A.; Musaev, D. G.; Hill, C. L. *Angew. Chem., Int. Ed.* **2008**, *47*, 3896. (n) Morris, N. D.; Suzuki, M.; Mallouk, T. E. *J. Phys. Chem. A* **2004**, *108*, 9115.

(3) See Supporting Information for synthetic procedures.

(4) Measurements over longer periods are now in progress using a headspace oxygen detector.

(5) Yagi, M.; Sukegawa, N.; Kaneko, M. *J. Phys. Chem. B* **2000**, *104*, 4111.

(6) Gilbert, J. A.; Eggleston, D. S.; Murphy, W. R., Jr.; Geselowitz, D. A.; Gersten, S. W.; Hodgson, D. J.; Meyer, T. J. *J. Am. Chem. Soc.* **1985**, *107*, 3855.

(7) Yagi, M.; Tomita, E.; Kuwabara, T. *J. Electroanal. Chem.* **2005**, *579*, 83.

(8) DFT(B3LYP) calculations are carried out with Gaussian03 (full reference in the SI). The geometry of $[(Cp^*)Ir(O)(ppy)]^+$ is fully optimized for each spin state with basis set I (Stuttgart−Bonn scalar relativistic ECP with associated basis set for Ir and 6-31G** for O, N, C, and H). The zero-point and entropy energy corrections are obtained from gas phase frequency calculations with basis set I, as the difference between the potential and free energies, $(G-E)_g$. The energies in solution, G_{sol}, are obtained from single-point CPCM(H_2O) calculations with basis set II (the same as I but with 6-311+G** for O, N, C, and H). The energies given in the text are obtained by adding G_{sol} to $(G-E)_g$.

(9) (a) Schilling, B. E. R.; Hoffmann, R.; Faller, J. W. *J. Am. Chem. Soc.* **1979**, *101*, 592. (b) Kiel, W. A.; Lin, G. Y.; Constable, A. G.; McCormick, F. B.; Strouse, C. E.; Eisenstein, O.; Gladysz, J. A. *J. Am. Chem. Soc.* **1982**, *104*, 4865.

(10) Lundberg, M.; Blomberg, M. R. A.; Siegbahn, P. E. M. *Inorg. Chem.* **2004**, *43*, 264.

(11) Yang, X.; Baik, M.-H. *J. Am. Chem. Soc.* **2008**, *130*, 16231.

JA901270F